DALTON
FULL PAPER

Structures of $Ga(hfac)_3$ and $In(hfac)_3$ (hfac = 1,1,1,5,5,5-hexafluoropentane-2,4-dionate) in the gas phase as studied by electron diffraction and *ab initio* calculations †

Paul T. Brain,[a] Michael Bühl,[b] Heather E. Robertson,[a] Andrew D. Jackson,[c] Paul D. Lickiss,[c] Donald MacKerracher,[b] David W. H. Rankin,*[,a] Dipti Shah[c] and Walter Thiel[b]

[a] *Department of Chemistry, University of Edinburgh, West Mains Road, Edinburgh, UK EH9 3JJ*
[b] *Institut für Organische Chemische, Universität der Zürich, Winterthurerstrasse 190, CH-8057, Zürich, Switzerland*
[c] *Department of Chemistry, Imperial College of Science, Technology and Medicine, South Kensington, London, UK SW7 2AY*

The molecular structures of $Ga(hfac)_3$ and $In(hfac)_3$ (hfac = 1,1,1,5,5,5-hexafluoropentane-2,4-dionate) have been determined by gas-phase electron diffraction (GED) restrained by *ab initio* computations. The structures, with D_3 symmetry, have a distorted octahedral arrangement of oxygen atoms about the central atom such that the E(hfac) planes are orientated at *ca*. 82 (E = Ga) and 81° (E = In) to one another. Theoretical computations at the SCF and DFT levels afford structures similar to those found experimentally but with less distorted EO_6 octahedra, *ca*. 89 and 87° (DFT), respectively.

The potential use of $CuInSe_2$ and $CuIn_xGa_{(1-x)}Se_2$ as high efficiency, radiation hard photovoltaic materials is now widely recognised,[1,2] but although a range of methods such as thermal evaporation, electron beam evaporation, and radio-frequency (r.f.), direct-current (d.c.) and magnetron sputtering have been used for their preparation, such techniques have not proved to be ideal with regard to reproducibility and control.[2] Chemical vapour deposition (CVD) is a well established technique in the semiconductor industry and is able to offer a good means of control of material composition and reproducibility, and in past years it has been applied to the deposition of Cu, In and Se for the preparation of thin films of $CuInSe_2$.[3–5] One of the areas of significant interest in the field of CVD is the development of new precursors for the various elements to be deposited[6–8] and substituted pentane-2,4-dionate (acetylacetonate) derivatives of a range of metals have become popular because of their stability under normal conditions, their volatility, and their ability to deposit metals cleanly under relatively mild conditions.[3,4,6,7] It thus became of interest to determine the structures of some of these potentially useful precursors in the gas phase, in which they are used for CVD purposes.

Experimental

Synthesis

The synthesis of both $Ga(hfac)_3$ and $In(hfac)_3$ (hfac = 1,1,1,5,5,5-hexafluoropentane-2,4-dionate) from the reaction between Hhfac and the appropriate metal nitrate has been reported previously.[9] However, in this work the method used involved the reaction between Na(hfac)[10] and the metal trichloride. Thus $Ga(hfac)_3$ and $In(hfac)_3$ were both prepared as white solids in yields of 85 and 57%, respectively. The melting point for $Ga(hfac)_3$ was found to be 66–67.5 °C (lit.,[9] 68.5–70 °C) and for $In(hfac)_3$ 69–72 °C (lit.,[9] 73 °C). Selected, previously unreported spectroscopic data, for $Ga(hfac)_3$: δ(^{13}C) 92.79 (CH), 116.54 (q, $^1J_{CF}$ = 283.5, CF_3), 182.42 (q, $^2J_{CF}$ = 37.8 Hz, CO); IR 1652w, 1622m, 1575m, 1548m, 1270m, 1255w, 1217m, 1146m, 1105w, 954w, 829m, 816s, 774m, 749m, 738w, 673s, 590s cm^{-1}; for $In(hfac)_3$: δ(^{13}C) 92.98 (CH), 116.51 (q, $^1J_{CF}$ = 284.3), 183.93 (q, $^2J_{CF}$ = 37.4 Hz); *m/z* 736 (15, $[M]^+$), 667 (20, $[M - CF_3]^+$), 529 (100, $[M - hfac]^+$), 479 (52, $[M - hfac - CF_2]^+$), 341 (37, $[M - hfac - 2CF_3 - CF_2]^+$ 291 (14, $[M - hfac - 2CF_3 - 2CF_2]^+$), 139 (12, $[Hhfac - CF_3]^+$), 115 (30, $[In]^+$), 69 (31%, $[CF_3]^+$).

Electron-diffraction measurements

Electron-scattering intensities were recorded on Kodak Electron Image plates using the Edinburgh gas-diffraction apparatus operating at *ca*. 44.5 kV (electron wavelength *ca*. 5.7 pm).[11] Nozzle-to-plate distances were *ca*. 95 and 258 mm, yielding data in the s range 20–356 nm^{-1}; three usable plates were obtained at each distance. The sample and nozzle were held respectively at *ca*. 403 and 428 K for $Ga(hfac)_3$, and 414 and 437 K for $In(hfac)_3$, during the exposure periods.

The scattering pattern of benzene was also recorded for the purpose of calibration; this was analysed in exactly the same way as those of the hfac compounds so as to minimise systematic errors in the wavelengths and camera distances. Weighting functions used to set up the off-diagonal weight matrices, correlation parameters, final scale factors and electron wavelengths are detailed in Table 1.

The electron-scattering patterns were converted into digital form using a computer-controlled Joyce-Loebl MDM6 microdensitometer with a scanning program described previously.[12] The programs used for data reduction[12] and least-squares refinement[13] have been described elsewhere; the complex scattering factors employed were those listed by Ross *et al*.[14]

Computational details

Geometries have been optimised at the SCF (Hartree–Fock self-consistent field) level[15] employing a polarised valence triple-zeta basis for Ga (a contracted 6s5p2d + d-polarisation basis, denoted TZVP),[16] the relativistic Hay–Wadt pseudopotential together with a polarised double-zeta valence basis for

† *Supplementary data available*: Cartesian coordinates for the experimental and theoretical structures and a list of the restraints. For direct electronic access see http://www.rsc.org/suppdata/dt/1998/545/, otherwise available from BLDSC (NO. SUP 57333, 11 pp.) or the RSC Library. See Instructions for Authors, 1998. Issue 1 (http://www.rsc.org/dalton).

Table 1 Nozzle-to-plate distances, weighting functions, correlation parameters, scale factors and electron wavelengths for the GED analysis

Compound	Camera distance/mm	Weighting functions/nm^{-1} Δs	s_{min}	s_1	s_2	s_{max}	Correlation parameter	Scale factor, k [a]	Electron wavelength [b]/pm
$Ga(hfac)_3$	95.17	4	100	120	304	356	0.2910	0.632(31)	5.706
	257.27	2	40	60	140	164	−0.0938	0.751(11)	5.707
$In(hfac)_3$	95.10	4	100	120	304	356	−0.0416	0.718(27)	5.679
	257.98	2	40	60	140	164	0.1158	0.717(8)	5.681

[a] Figures in parentheses are the estimated standard deviations (e.s.d.s). [b] Determined by reference to the scattering patterns of benzene vapour.

Table 2 Structural parameters (r_a/pm, $\angle_a$/°)* for the GED refinements

Number	Parameter	$Ga(hfac)_3$	$In(hfac)_3$
1	$[2r(C–O) + 6r(C–F) + 2r(C–C_{ring}) + 2r(C–C_F)]/12$	136.4(1)	136.4(1)
2	$r(C–C_F) - [2r(C–O) + 6r(C–F) + 2r(C–C_{ring})]/10$	19.2(5)	19.6(4)
3	$r(C–C_{ring}) - [2r(C–O) + 6r(C–F)]/8$	6.6(6)	7.6(7)
4	$r(C–F) - r(C–O)$	7.5(8)	8.7(5)
5	$r(E–O)$	194.5(4)	212.5(5)
6	$r(C–H)$	109.4(19)	109.3(18)
7	$\angle(O–E–O)$	90.3(4)	84.8(4)
8	$\angle(E–O–C)$	127.8(6)	126.4(6)
9	$\angle(O–C–C_F)$	114.1(5)	114.1(5)
10	$\angle(C–C–F)$	111.2(2)	110.6(3)
11	∠[O–C–C–F(11)]	38.5(11)	41.1(12)
12	∠('D_3 twist')	49.9(4)	48.4(4)

* For definitions of parameters and conditions for the refinements, see the text. Values in parentheses are the estimated standard deviations.

In (contracted to 2s2p + d-polarisation, d exponent 0.15),[17] and 6-31G* basis[15] for all other elements. The complete basis for all atoms is referred to as "6-31G*". The geometries have been re-optimised at a gradient-corrected level of DFT (density-functional theory)[18] employing Becke's 1988[19] and Perdew's 1986[20] exchange-correlation functionals (denoted BP86), together with the same basis as above and a medium-sized grid (grid 3[21]). For the Ga compounds, harmonic vibrational frequencies and electric field gradients (EFGs) have been computed at the SCF level for the SCF geometries using the same basis set. Optimisations have been performed using the TURBOMOLE package[22] with the DFT implementation;[21] the frequency and EFG computations have employed the GAUSSIAN suite of programs.[23] The optimisation of geometries using Møller–Plesset theory (*e. g*. at the MP2 level)[15] were too expensive in terms of the CPU time available to us.

For $Ga(hfac)_3$, the magnetic shielding tensor has been computed at the GIAO (gauge-including atomic orbitals)-SCF level[24] employing the SCF geometry above and the following, contracted Ahlrichs basis set of essentially TZP (polarised triple-zeta) quality:[25] Ga (14s11p5d) contracted to [9s7p3d] ‡ and augmented with one d-polarisation function (exponent 0.207); C,O,F (10s/6p)/[6s3p] with one d-polarisation function (exponents 0.1, 1.0, and 1.4 for C, N, and F, respectively); H (5s)/[3s] with one p-polarisation function (exponent 0.8). These calculations have been performed with TURBOMOLE (direct implementation).[26] Absolute Ga shieldings have been converted into chemical shifts using a reference shielding value of 1946.7 ppm, as evaluated from a σ_{calc} *vs*. δ_{expt} correlation for a large number of Ga compounds (SCF//SCF level).[27]

Molecular models

The *ab initio* computations predict a minimum on the potential-energy surfaces for $Ga(hfac)_3$ and $In(hfac)_3$ having D_3 symmetry, and this overall symmetry was assumed throughout the GED refinements. Additionally, local C_{3v} symmetry was assumed for the $C–CF_3$ groups, defining the atomic coordinates for both $Ga(hfac)_3$ and $In(hfac)_3$ by a model consisting of the 12 independent parameters listed in Table 2. With reference to Fig. 1, the distance parameters were: the mean of all non-hydrogen bonding distances in the hfac ligands, p_1; the difference between the $C–CF_3$ distance and the other non-hydrogen bonding distances in hfac, p_2; the difference between the C–C distance in the ring and a weighted mean of the C–O and C–F distances, p_3; the difference between the C–O and C–F distances, p_4; the central metal (E) to oxygen distance, p_5; and the C–H distance, p_6. The other six parameters consisted of four bond angles and two torsion angles: O–E–O, p_7; E–O–C, p_8; O–C–CF_3, p_9; C–C–F, p_{10}; O–C–C–F(11), p_{11}, defining the clockwise rotation of the CF_3 groups about $C–CF_3$ away from a starting position with one C–F bond *syn* to the ring O–C bond; and the so-called 'D_3 twist' angle, p_{12}, a clockwise rotation of the hfac groups about their C_2 axes relative to a starting position with all oxygen atoms coplanar.

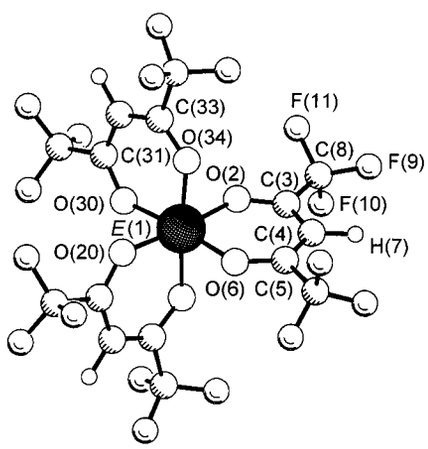

Fig. 1 Perspective view of the $E(hfac)_3$ geometry (E = Ga or In) with D_3 symmetry showing the numbering system used in the GED analysis

Refinement

The radial-distribution (RD) curves for $Ga(hfac)_3$ and $In(hfac)_3$ are shown in Fig. 2. They are similar to one another, demon-

‡ This basis has been decontracted from the Ga DZ basis.

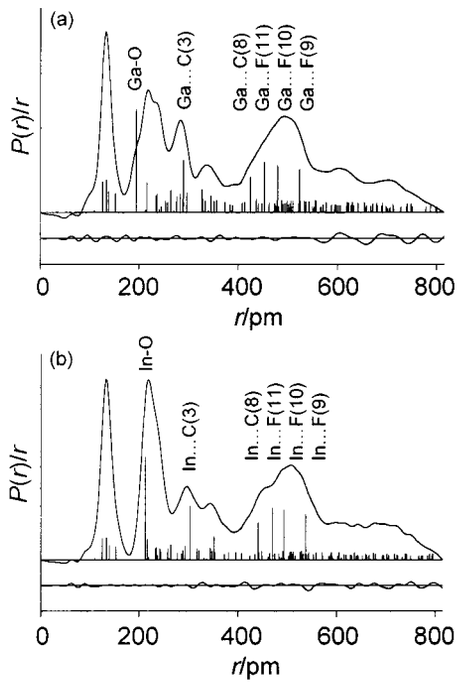

Fig. 2 Observed and final weighted difference radial-distribution curves for (a) $Ga(hfac)_3$ and (b) $In(hfac)_3$. Before Fourier inversion the data were multiplied by $s\cdot\exp[(-0.000\,02s^2)/(Z_E - f_E)(Z_o - f_o)]$ (E = Ga and In, respectively)

strating an intense peak at *ca*. 135 pm, three broad peaks lying between 200 and 400 pm, and a very broad feature between 400 and 500 pm. Above 550 pm, the RD curve consists of a relatively intense but featureless continuum.

From the bar lines in the RD curves, for which the height of each is proportional to the area of the distance peak, it is clear that no peak is associated with a single distance. Thus, the peak at 135 pm represents scattering from all bonded, light-atom (*i.e*. excluding Ga or In) interatomic pairs in the hfac groups, *viz*. C–H, C–O, C–F, $C–C_{ring}$ and $C–C_F$. The predominant scattering in these compounds arises from the bonded *E*–O distances and forms the major component of the peak at *ca*. 225 pm, together with scattering from two-bond F···F pairs; for $Ga(hfac)_3$, the Ga–O distance is resolved partially as a shoulder near 200 pm. The feature at 225 pm also includes contributions from two-bond, light-atom scattering [O(2)···C(4)/C(8), C(3)···C(5)/F(9)/F(10)/F(11) and C(4)···C(8)], appearing as a distinct shoulder at *ca*. 240 pm in the $Ga(hfac)_3$ curve. The broad peak centred at *ca*. 290 pm is associated mainly with scattering from the two-bond *E*···C(3) pairs, whilst that at *ca*. 340 pm consists of scattering from the three-bond pairs *E*···C(4), O(2)···F(9)/C(33)/[C(31) for $Ga(hfac)_3$] and C(4)···F(11)/[F(10) for $Ga(hfac)_3$]. The broad feature spanning the range 400–550 pm is attributable principally to scattering from the three-bond *E*···C(8) pairs and to the four-bond *E*···F pairs. At $r > 400$ pm, the RD curves consist of an almost continuous range of non-bonded distances (up to eight-bond F···F pairs) which, being mostly non-hydrogen distances, contribute significant scattering intensity.

The r_a structure of the hfac compounds was refined. For $Ga(hfac)_3$, a harmonic vibrational force field was computed at the SCF/"6-31G*" level and the Cartesian force constants were transformed into those described by a set of symmetry coordinates using the program ASYM*X*.[28] As a full analysis of experimental vibrational frequencies is not available for the compound, it was not possible to scale the theoretical force constants on this basis. Instead, as the best alternative, empirical scale factors of 0.9 for bond stretches, 0.85 for bends and 0.8 for out-of-plane bends and torsions were employed.[29] Values for the root-mean-square amplitudes of vibration (u) were then derived from the scaled force constants using ASYM*X*. The presence of 25 low frequency modes ($\nu < 200$ cm^{-1}, 12 of which having $\nu < 100$ cm^{-1}) gave unrealistically large values of K and precluded the possibility of refining r_a^o structures for the compounds.

For $In(hfac)_3$, the use of a pseudo-potential on the In atom precluded the possibility of an analytical frequency computation using GAUSSIAN 94. Further, the CPU expense of a numerical frequency computation allowed us only to compute a vibrational force field at the SCF/"3-21G*" level. The same level of force field was computed for $Ga(hfac)_3$ to permit comparison of the derived u values with those at the SCF/"6-31G*" level. From this comparison, a set of consistent scaling constants suitable for the $In(hfac)_3$ force field was derived. These constants were 0.8 for bond stretches, 0.75 for bends and 0.7 for out-of-plane bends and torsions.

Starting values for the twelve geometric parameters were taken from the *ab initio* computations. Subsequent refinements for each compound showed that such values derived from the SCF/"6-31G*" and BP86/"6-31G*" level calculations yielded the same final structure. In the initial refinements the hfac difference parameters, p_2–p_4, and the C–H bond distance, p_6, were fixed at the BP86/"6-31G*" values whilst all of the other geometrical parameters were refined. For $In(hfac)_3$, refinement of the $O–C–C_F$ angle, p_9, resulted in an unstable refinement and an unrealistically large value of the angle; it too was fixed in the initial refinements. Refinement of amplitudes of vibration pertaining to the most intense scattering pairs allowed subsequent refinement of parameters p_2–p_4 for both compounds. However, this was possible only if flexible restraints were applied to the $C–C_{ring}$ and $C–C_F$ bond distances.[30]

The introduction of flexible restraints by the 'SARACEN' method[30] may allow the refinement of parameters which would otherwise have to be fixed. Estimates of the values of these restrained quantities and their uncertainties are used as additional observations in combined analyses similar to those routinely carried out for electron-diffraction data combined with rotation constants and/or dipolar coupling constants.[31] The values and uncertainties for the extra observations are derived from other methods such as X-ray diffraction or theoretical computations. *All* geometrical parameters are then included in the refinements. In cases where a restraint corresponds exactly to a refined parameter, if the intensity pattern contains useful information concerning the parameter, it will refine with an e.s.d. less than the uncertainty in the corresponding additional observation. However, if there is essentially no relevant information, the parameter will refine with an e.s.d. equal to the uncertainty of the extra observation and its refined value will equal that of the restraint. In this case, the parameter can simply be fixed, in the knowledge that doing this does not influence either the magnitudes or the e.s.d.s of other parameters. In some cases, because increasing the number of refining parameters allows all effects of correlation to be considered, some e.s.d.s may increase. Overall, this approach utilises all available data as fully as possible and returns more realistic e.s.d.s for refining parameters; the unknown effects of correlation with otherwise fixed parameters are revealed and included.[32]

The $C–C_{ring}$ and $C–C_F$ bond distances were restrained with values of 139.6 and 153.8 pm respectively for $Ga(hfac)_3$ and 139.8 and 153.9 pm respectively for $In(hfac)_3$; each restraint was given an uncertainty of 0.8 pm. These values are averages of the bond distances computed at the SCF and BP86 levels, whilst the uncertainties are half the differences. This reflects our experience of such calculations (values of these types of distance are often underestimated at SCF but overestimated at DFT levels), and thus these values are the most realistic estimates given the resources available to us.

Of the 157 different distances in each molecule, the majority

Table 3 Selected distances (r_a/pm) from the GED analyses[a]

		$Ga(hfac)_3$		$In(hfac)_3$	
Number	Atom pair[b]	Distance	Amplitude	Distance	Amplitude
1	*E*(1)–O(2)	194.5(4)	7.5(4)	212.5(5)	7.2(5)
2	O(2)–C(3)	126.2(7)	3.9(4)	125.1(5)	4.1(4)
3	C(3)–C(4)	138.4(5)	4.5(4)	139.2(6)	4.7(4)
4	C(3)–C(8)	152.4(5)	5.2(5)	152.7(4)	5.6(4)
5	C(8)–F	133.7(2)	4.0(3)	133.8(2)	4.4(3)
6	*E*(1) · · · C(3)	289.6(5)	7.1(4)	303.8(6)	7.9(6)
7	O(2) · · · C(4)	234.7(10)	5.8(5)	242.0(9)	7.2(6)
8	O(2) · · · C(8)	234.2(7)	8.8(8)	233.6(8)	7.0(7)
9	O(2) · · · C(6)	275.9(13)	9.0 (tied to u_6)	286.6(15)	10.8 (rf)
10	C(3) · · · F(9)	236.3(6)	7.2(4)	235.7(5)	7.0(4)
11	C(3) · · · F(10/11)	236.3(6)	7.9 (tied to u_{10})	235.7(5)	8.0 (tied to u_{10})
12	C(4) · · · C(8)	253.2(9)	7.3 (tied to u_7)	244.1(9)	7.0(6)
13	F · · · F (two bond)	215.9(2)	5.7(3)	217.0(3)	6.6(2)
14	O(2) · · · O(20)	388.7(7)	9.9(f)	424.9(11)	10.2 (f)
15	O(2) · · · O(30)	283.0(21)	11.5 (tied to u_6)	317.8(25)	14.0(12)
16	O(2) · · · O(34)	258.2(39)	13.4 (rf)	277.7(52)	15.8(15)
17	*E*(1) · · · C(4)	327.0(11)	7.8 (rf)	351.9(11)	8.3 (rf)
18	*E*(1) · · · C(8)	424.7(6)	9.4(7)	441.2(6)	11.2(8)
19	O(2) · · · F(9)	345.2(5)	7.0 (rf)	344.5(5)	7.6(6)
20	O(2) · · · F(10)	297.0(13)	17.5(16)	293.4(14)	20.0(17)
21	O(2) · · · F(11)	264.5(10)	17.3(16)	264.6(10)	19.6(17)
22	*E*(1) · · · F(9)	523.1(5)	10.3(7)	537.5(7)	11.3(7)
23	*E*(1) · · · F(10)	479.9(12)	19.4(15)	493.5(13)	18.0(15)
24	*E*(1) · · · F(11)	452.5(10)	13.4(11)	470.2(10)	16.1(12)

[a] Values in parentheses are the estimated standard deviations: rf = refined then fixed; f = fixed. [b] For atom-numbering scheme, see Fig. 1. All other distances were included in the refinements but are not shown here.

Table 4 Correlation matrices (× 100)* for (a) $Ga(hfac)_3$ and (b) $In(hfac)_3$

(a)

p_7	p_9	p_{10}	
	52		p_3
−55		60	p_4
−81	55		p_8

(b)

p_8	p_9	p_{10}	
		69	p_5
−83			p_7
	65		p_8

* Only elements with absolute values > 50 are shown.

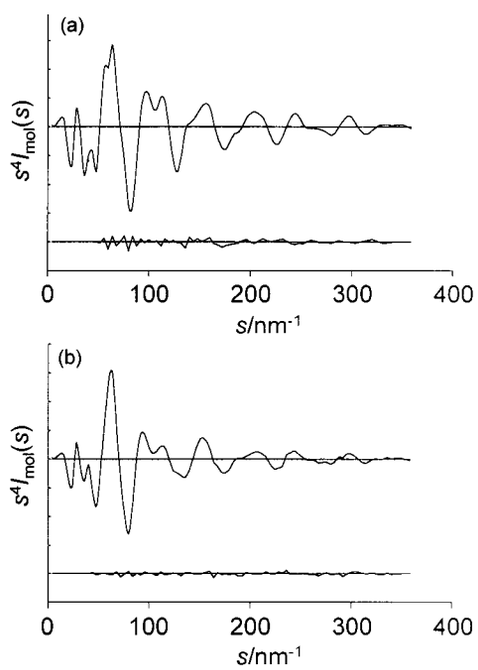

Fig. 3 Observed and final weighted difference combined molecular-scattering intensity curves for (a) $Ga(hfac)_3$ and (b) $In(hfac)_3$. Theoretical data are shown where experimental data were not available

contribute a scattering intensity at least 5% of the principal (*E*–O) scattering pairs. It was important therefore to explore the simultaneous refinement of as many of the associated amplitudes of vibration as possible, either independently or tied together in groups. This was found to be best achieved by introducing flexible restraints for all refining amplitudes with values from the computed force fields, allowing a 10% uncertainty for each. In this way it was possible to refine 86 and 83 amplitudes simultaneously in the $Ga(hfac)_3$ and $In(hfac)_3$ refinements, respectively. Of course, the majority of these were determined almost entirely by the restraints, returning e.s.d.s and values very similar to those of their restraints. In such cases, these amplitudes were fixed in the final refinements provided that they were not correlated significantly with other refining parameters (≤10% in the correlation matrices, Table 4), and thus did not contribute to their e.s.d.s. A total of 31 (*E* = Ga) and 35 (*E* = In) amplitudes were refined, respectively. This process allowed us to be sure that the quoted e.s.d.s of refining parameters are the most realistic estimate of the uncertainties in the electron-diffraction experiment.

Attempts to refine the angle O–C–C_F, p_9, in $In(hfac)_3$ unrestrained were unsuccessful, as were attempts to refine r(C–H), p_6, in either compound. These geometric parameters were refined using flexible restraints of 113.0 ± 1.0° and 108.8 ± 2.0 pm, respectively.

Values of the principal interatomic distances for the final refinements ($R_G = 0.085$ and $R_D = 0.092$, *E* = Ga; $R_G = 0.067$ and $R_D = 0.061$, *E* = In) are listed in Table 3 and the most significant values of the least-squares correlation matrices are given in Table 4. The experimental and difference radial-distribution curves are shown in Fig. 2 and the molecular-scattering intensities in Fig. 3. Cartesian coordinates for the experimental and theoretical structures are given in SUP 57333, together with a list of the restraints.

Table 5 A comparison of theoretically optimised and experimentally determined[a] geometrical parameters (r/pm, ∠/°)

	$Ga(hfac)_3$				$In(hfac)_3$		
Parameter[b]	SCF/"6-31G*"	BP86/"6-31G*"	GED	X-ray[c]	SCF/"6-31G*"	BP86/"6-31G*"	GED
$r(E–O)$	196.6	199.5	194.5(4)	195.4(5)[d]	207.8	211.6	212.5(5)
$r(O–C)$	124.3	128.1	126.2(7)	125(1)[d]	124.3	128.0	125.1(5)
$r(C–C_{ring})$	138.8	140.3	138.4(5)	138(1)[d]	139.0	140.5	139.2(6)
$r(C–C_F)$	153.0	154.5	152.4(5)	152(1)[d]	153.1	154.6	152.7(4)
$r(C–F)$	131.5[d]	135.4[d]	133.7(2)	129(2)[d]	131.6[d]	135.5[d]	133.8(2)
∠(E–O–C)	128.8	125.2	127.8(6)	125.5(5)[d]	130.3	127.3	126.4(6)
∠(O–E–O)	87.6	91.6	90.3(5)	91.0(2)[d]	83.3	86.3	84.8(4)
∠(O–C–C_F)	112.8	112.9	114.1(5)	113.6(5)[d]	112.8	113.0	114.1(5)
∠(C–C–F)	110.5[d]	110.6[d]	111.2(2)	112(1)[d]	110.5[d]	110.5[d]	110.6(3)
∠[O–C–C–F(11)]	60.0	60.2	38.5(11)	43.5(7)[d]	59.1	60.4	41.1(12)
∠('D_3 twist')	56.0	55.4	49.9(4)	54.7[e]	57.1	56.9	48.4(4)

[a] Values in parentheses are the estimated standard deviations. [b] For atom-numbering scheme, see Fig. 1; for definitions of parameters see the text. [c] Ref. 33. [d] Average value. [e] Average of approximate values.

Results and Discussion

GED structures of $Ga(hfac)_3$ and $In(hfac)_3$

The electron scattering patterns of $Ga(hfac)_3$ and $In(hfac)_3$ are consistent with molecular geometries having D_3 symmetry. The six oxygen atoms surrounding the central E atoms define a distorted octahedral co-ordination such that the E(hfac) planes are orientated at *ca.* 83° (E = Ga) and *ca.* 81° (E = In) to one another. Since the In–O distance at 212.5(5) pm is longer than Ga–O at 194.5(4) pm, the hfac 'bite' angle (O–E–O) is wider in $Ga(hfac)_3$, at 90.3(4)°, than in $In(hfac)_3$, at 84.8(4)°. However, the hfac units in each compound may be regarded otherwise as identical; a comparison of the geometrical parameters defining the hfac groups for each shows them all to be within 2 e.s.d.s of one another (Tables 2 and 5).

Results of the *ab initio* computations are given in Table 5. For both $Ga(hfac)_3$ and $In(hfac)_3$, changing from the SCF to the DFT level results in a significant increase in the bond lengths, whilst the angles E–O–C and O–E–O become significantly narrower and wider, respectively. At each level, parameters relating to the hfac units, notwithstanding angles O–E–O, are effectively identical when comparing the Ga and In structures.

For $Ga(hfac)_3$, the theoretically optimised geometries may be compared with both the gas- and solid-state[33] structures, parameters for the latter also being shown in Table 5. The bonded distances in the SCF optimised geometry agree quite well with the experimental values.§ In contrast, the BP86 optimised bond distances are consistently overestimated; compare, in particular, the Ga–O distances of 196.6 (SCF), 199.5 (BP86), 195.4(5) (X-ray),[33] and 194.5(4) pm (GED). In $Ga(acac)_3$ (s) (acac = pentane-2,4-dionate), the average Ga–O bond length, determined by X-ray diffraction, is 195.2(6) pm.[34] A similar tendency for bond length overestimation by DFT methods associated with the 6-31G* basis set has been noted for compounds of first-row elements.[35] For many of these compounds, DFT optimised parameters have been found to improve upon improvement of the basis set;[36] the same would probably hold for the molecules in this study. Interestingly, and in contrast, the In–O bond length is underestimated at both the SCF (207.8 pm) and DFT (211.6 pm) levels [GED, 212.5(5) pm], albeit only slightly at DFT/"6-31G*". This may reflect the use of a relativistic pseudo-potential for indium in the computations for $In(hfac)_3$. Only six compounds containing In(acac) groups have been structurally characterised, all by single-crystal X-ray diffraction.[37–42] Excluding the dimeric structure of dimethyl(salicylaldehyde)indium,[42] the In–O bond distances range from 210.8 to 216.3 pm, consistent with the gas-phase structure of $In(hfac)_3$ found in this study.

Notwithstanding the E–O distances, the most notable differences between the experimentally determined and the theoretically predicted parameters lie with the dihedral angles, O–C–C–F(11) and the 'D_3 twist'. In the GED refinements, the rotation of the CF_3 group has been assumed to give rise to a single conformation, *i.e.* a static description has been used. However, the predicted low frequency (<100 cm^{-1}) of the modes describing the CF_3 rotation about $C–C_F$ indicates that this motion is described by a very flat potential-energy function. The GED refined values of 38.5(11)° (E = Ga) and 41.1(12)° (E = In) represent the best fit with a static model to this motion time-averaged over the duration of the experiment, and do not necessarily imply that the gas-phase structure has angles different from the theoretically predicted equilibrium position of *ca.* 60° for O–C–C–F(11). In the solid-state structure of $Ga(hfac)_3$[33] the average value of O–C–C–F(11) was determined to be 43.5(7)°. This further supports the idea of a very low barrier to rotation of the CF_3 group, this non-equilibrium conformation being brought about by the action of intermolecular packing forces present in the solid state.

The refined value of the 'D_3 twist' angle in the gas-phase structures is *ca.* 6° lower for $Ga(hfac)_3$ and *ca.* 8° lower for $In(hfac)_3$ than in the *ab initio* optimised structures (Table 5). These angles correspond to a closest non-bonded O···O distance of 258.2(39) pm in $Ga(hfac)_3$ and 277.7(52) pm in $In(hfac)_3$, *c.f.* SCF/"6-31G*" distances of 278.9 pm and 298.7 pm, respectively. In the solid-state structure of $Ga(hfac)_3$,[33] the shortest O···O distance falls at 271.2(8) pm. This disagreement, between the value for the GED refinement and those for the *ab initio* computations and the solid-state determination, is, at least superficially, surprising.

Differences between structures determined by different methods must be interpreted with care, particularly with regard to the effects of vibrational motion. The GED r_a refinements define a structure averaged over all vibrational motions; no allowance for the effects of shrinkage has been undertaken for comparison with the *ab initio* equilibrium (r_e) structure. A large-amplitude twisting motion of the hfac groups about the C_2 axes would give rise to such a shrinkage effect. The vibrational mode associated with this motion is predicted (SCF/"6-31G*" level) to lie at *ca.* 167 cm^{-1}, commensurate with a large torsional amplitude. A geometry optimised with the 'D_3 twist' angle held at 50° lies *ca.* 16 kJ mol^{-1} higher in energy than the fully optimised structure at the SCF/"6-31G*" level (Table 6). At the BP86/"6-31G*" level, this difference is reduced substantially, the 50° twisted conformation being predicted to lie at 9.5 kJ mol^{-1} above the minimum. The DFT energy difference is *ca.* 2.6RT (T = 428 K) and implies only a small contribution from such conformations to the GED scattering pattern, *i.e.* the

§ It should be borne in mind that experimental and theoretical distances are not expected to be identical; the experimental structure is averaged over all vibrational motions whilst the theoretical structure corresponds to the minimum on the potential-energy surface.

Table 6 GIAO-SCF chemical-shift calculations[a] for $Ga(hfac)_3$

Geometry	$\delta(^{71}Ga)$/ppm[b]	E(rel)[c]/kJ mol^{-1}
SCF/"6-31G*"	−7	0.0
DFT/"6-31G*" (full)[d]	−22	161.7
DFT/"6-31G*" (50°)[e]	−22	177.6[f]
GED	19	94.0

[a] Computed at the SCF/TZP level. [b] Relative to Ga^{3+}(aq). [c] Energy relative to the SCF/"6-31G*" fully optimised geometry. [d] Geometry fully optimised. [e] Geometry optimised whilst holding the 'D_3 twist' angle fixed at 50°. [f] At the BP86/"6-31G*" level, the 50° twisted conformation lies 9.5 kJ mol^{-1} above the fully optimised structure.

amplitude of torsional vibration is not large enough to explain the difference between theory and experiment. However, it is possible that this energy difference would become smaller at higher levels of theory and the associated vibrational shrinkage effect would then be significant, accounting, at least in part, for the smaller value of the 'D_3 twist' in the GED structure compared to the present theoretical predictions.

Unlike the GED and theoretical structures with D_3 symmetry, the solid-state structure of $Ga(hfac)_3$ has a distorted, C_1, geometry.[33] This low symmetry is manifested particularly in the range of dihedral parameters describing the hfac groups: O–C–C–F(11), *ca*. 25–56°; 'D_3 twist', *ca*. 53.8–55.6°; angle between planes OGaO/CCC, 2.5–10.3°. Such distortions are associated with the action of intermolecular forces upon motions in the molecule having relatively shallow potential-energy functions. The solid-state structure thus represents a summation of both intramolecular and intermolecular forces, yielding the small differences relative to the gas-phase structure.

The ^{71}Ga NMR shift for $Ga(hfac)_3$

Very recently, ^{71}Ga chemical shifts computed *ab initio* have been assessed in detail.[27] Nuclear magnetic resonance spectroscopy of ^{69}Ga, and to a lesser extent ^{71}Ga, is hampered by quadrupolar line broadening, which can give rise to undetectably broad signals.[43] According to the theory of quadrupolar relaxation,[44] the line width $\Delta\nu_{\frac{1}{2}}$ should be proportional to q_{zz}^2 (*i.e*. the square of the largest component of the EFG tensor) and to τ_c, the molecular correlation time. For a number of ^{91}Zr and ^{71}Ga resonances,[45,27] trends in experimental line widths have been found to be consistent with changes in the computed value of q_{zz}^2. Theoretical (or experimental where available) EFGs are thus a measure of the reduction in symmetry around the nucleus that is frequently associated with extremely broad lines, *e.g*. for ^{71}Ga resonances. In order to test if $Ga(hfac)_3$ might lend itself to characterisation *via* ^{71}Ga NMR spectroscopy, the line width has now been predicted on the basis of the computed EFGs.

For the $Ga(acac)_3$, experimental line widths vary between 1090 (T = 85 °C) and 2600 (T = 26 °C) Hz,[46] and a $\delta(^{71}Ga)$ value of −14 ppm has been reported.[47]¶ For this molecule, the experimentally deduced EFG, 25.4 10^{20} V m^{-2},[47] has been reproduced reasonably well at the SCF level, 22.3 10^{20} V m^{-2}.[27] A slightly larger value is predicted for $Ga(hfac)_3$, 24.2 10^{20} V m^{-2}. Assuming the same correlation times as for $Ga(acac)_3$, line widths between 1280 (85 °C) and 3060 (26 °C) Hz are predicted for $Ga(hfac)_3$, based on the data for the acac parent. The value of τ_c depends on the reorientational mobility of a molecule and increases with its size. Therefore, τ_c should be somewhat larger for $Ga(hfac)_3$ than for $Ga(acac)_3$, and the predicted line widths for the former should be regarded as lower limits. However, the ^{71}Ga NMR signal of $Ga(hfac)_3$ should be detectable, in particular at higher temperatures.

¶ Recording these spectra is not routine, as witnessed by another group's unsuccessful attempt to detect the ^{71}Ga NMR resonance of $Ga(acac)_3$.[48]

The SCF//SCF computed ^{71}Ga chemical shift of $Ga(acac)_3$, −13 ppm, is in excellent agreement with experiment, also −13 ppm.[47] As expected, a very similar $\delta(^{71}Ga)$ value is predicted for $Ga(hfac)_3$, −7 ppm at the SCF//SCF level (Table 6) (+22 ppm for the final GED geometry at the same level). Thus, the signal is expected to occur close to that of the experimental standard, Ga^{3+}(aq), but the resonances should be discernible by their line widths.

Acknowledgements

We thank the EPSRC for financial support of the Edinburgh Electron Diffraction Service (grant GR/K44411), including research fellowships to P. T. B. and H. E. R., for studies at Imperial College under the 'Synthesis and Evaluation of Materials for the 21st Century' initiative, grant GR/H05609, and for provision of the microdensitometer facilities at the Daresbury Laboratory. We acknowledge Dr. L. Hedberg (Oregon State University) for the original copy of the program ASYM40, Dr. V. Typke (University of Ulm) for the variable-array version, and Dr. S. Parsons (University of Edinburgh) for accessing data from the Cambridge Database. M. B. thanks the Fonds der Chemischen Industrie for support. The *ab initio* calculations have been carried out on IBM RS/6000 workstations at the University and at the ETH (C4 cluster), Zürich.

References

1 R. F. Service, *Science*, 1996, **272**, 1745.
2 A. Rockett and R. W. Birkmire, *J. Appl. Phys.*, 1991, **70**, R81.
3 P. A. Jones, A. D. Jackson, P. D. Lickiss, R. D. Pilkington and R. D. Tomlinson, *Thin Solid Films*, 1994, **238**, 4.
4 P. A. Jones, A. D. Jackson, R. D. Pilkington and P. D. Lickiss, *Thin Solid Films*, 1993, **229**, 5.
5 A. D. Jackson, P. A. Jones, P. D. Lickiss and R. D. Pilkington, *J. Mater. Chem.*, 1993, **3**, 429.
6 M. J. Hampden-Smith and T. T. Kodas, *Chem. Vap. Deposition*, 1995, **1**, 8.
7 *The Chemistry of Metal CVD*, eds. T. Kodas and M. Hampden-Smith, VCH, Weinheim, 1994.
8 P. O'Brien and R. Nomura, *J. Mater. Chem.*, 1995, **5**, 1761.
9 K. Utsunomiya, *Bull. Chem. Soc. Jpn.*, 1971, **44**, 2688.
10 H.-K. Shin, K. M. Chi, J. Farkas, M. J. Hampden-Smith, T. T. Kodas and E. N. Duesler, *Inorg. Chem.*, 1992, **31**, 424.
11 C. M. Huntley, G. S. Laurenson and D. W. H. Rankin, *J. Chem. Soc., Dalton Trans.*, 1980, 954.
12 S. Cradock, J. Koprowski and D. W. H. Rankin, *J. Mol. Struct.*, 1981, **77**, 113.
13 A. S. F. Boyd, G. S. Laurenson and D. W. H. Rankin, *J. Mol. Struct.*, 1981, **71**, 217.
14 A. W. Ross, M. Fink and R. Hilderbrandt, in *International Tables for Crystallography*, ed. A. J. C. Wilson, Kluwer, Dordrecht, 1992, vol. C, p. 245.
15 W. Hehre, L. Radom, P. v. R. Schleyer and J. A. Pople, *Ab initio Molecular Orbital Theory*, Wiley, New York, 1986.
16 A. Schäfer, C. Huber and R. Ahlrichs, *J. Chem. Phys.*, 1994, **100**, 5829.
17 W. R. Wadt and P. J. Hay, *J. Chem. Phys.*, 1985, **82**, 284.
18 For example, see R. G. Parr and W. Yang, *Density Functional Theory of Atoms and Molecules*, Academic Press, Oxford, 1989.
19 A. D. Becke, *Phys. Rev. A*, 1988, **38**, 3098.
20 J. P. Perdew, *Phys. Rev. B*, 1986, **33**, 8822; **34**, 7406.
21 O. Treutler and R. Ahlrichs, *J. Chem. Phys.*, 1995, **102**, 346.
22 R. Ahlrichs, M. Bär, M. Häser, H. Horn and C. Kölmel, *Chem. Phys. Lett.*, 1989, **162**, 165.
23 M. J. Frisch, G. W. Trucks, H. B. Schlegel, P. M. W. Gill, B. G. Johnson, M. A. Robb, J. R. Cheesman, T. A. Keith, G. A. Petersson, J. A. Montgomery, K. Raghavachari, M. A. Al-Laham, V. G. Zakrzewski, J. V. Ortiz, J. B. Foresman, J. Cioslowski, B. B. Stefanov, A. Nanayakkara, M. Challacombe, C. Y. Peng, P. Y. Ayala, W. Chen, M. W. Wong, J. L. Andres, E. S. Replogle, R. Gomperts, R. L. Martin, D. J. Fox, J. S. Binkley, D. J. Defrees, J. Baker, J. J. P. Stewart, M. Head-Gordon, C. Gonzalez and J. A. Pople, GAUSSIAN 94, Gaussian Inc., Pittsburgh, PA, 1995.
24 R. Ditchfield, *Mol. Phys.*, 1974, **27**, 789; K. Wolinski, J. F. Hinton and P. Pulay, *J. Am. Chem. Soc.*, 1990, **112**, 8251.

25 A. Schäfer, H. Horn and R. Ahlrichs, *J. Chem. Phys.*, 1992, **97**, 2571.
26 M. Häser, R. Ahlrichs, H. P. Baron, P. Weiss and H. Horn, *Theor. Chim. Acta*, 1992, **83**, 455.
27 M. Bühl, *Magn. Reson. Chem.*, 1996, **34**, 782.
28 A variable-array version of the program ASYM20, L. Hedberg and I. M. Mills, *J. Mol. Spectrosc.*, 1993, **160**, 117. Program adaption from the ASYM40 version undertaken by V. Typke, University of Ulm, Germany.
29 For example, see, G. Rauhut and P. Pulay, *J. Phys. Chem.*, 1995, **99**, 3093, and refs. therein.
30 A. J. Blake, P. T. Brain, H. McNab, J. Miller, C. A. Morrison, S. Parsons, D. W. H. Rankin, H. E. Robertson and B. A. Smart, *J. Phys. Chem.*, 1996, **100**, 12 280; P. T. Brain, C. A. Morrison, S. Parsons and D. W. H. Rankin, *J. Chem. Soc.*, *Dalton Trans.*, 1996, 4589.
31 For example, see, B. T. Abdo, I. L. Alberts, C. J. Attfield, R. E. Banks, A. J. Blake, P. T. Brain, A. P. Cox, C. R. Pulham, D. W. H. Rankin, H. E. Robertson, V. Murtagh, A. Heppeler and C. Morrison, *J. Am. Chem. Soc.*, 1996, **118**, 209.
32 Also, see, B. A. Smart, L. E. Griffiths, C. R. Pulham, H. E. Robertson, N. W. Mitzel and D. W. H. Rankin, *J. Chem. Soc.*, *Dalton Trans.*, 1997, 1565; C. A. Morrison, B. A. Smart, S. Parsons, E. M. Brown, D. W. H. Rankin, H. E. Robertson and J. Miller, *J. Chem. Soc.*, *Perkin Trans. 2*, 1997, 857; P. T. Brain, D. W. H. Rankin, H. E. Robertson, M. A. Fox, R. Greatrex, A. Nikrahi and M. Bühl, *Inorg. Chem.*, 1997, **36**, 1048; P. T. Brain, B. A. Smart, H. E. Robertson, M. J. Davis, D. W. H. Rankin, W. J. Henry and I. Gosney, *J. Org. Chem.*, 1997, **62**, 2767; N. W. Mitzel, B. A. Smart, S. Parsons, H. E. Robertson and D. W. H. Rankin, *J. Chem. Soc.*, *Perkin Trans. 2*, 1996, 2727.
33 B. Ballarin, G. A. Battiston, F. Benetollo, R. Gerbasi, M. Porchia, D. Favretto and P. Traldi, *Inorg. Chim. Acta*, 1994, **217**, 71.
34 K. Dymock and G. J. Palenik, *Acta Crystallogr.*, *Sect. B*, 1974, **30**, 1364.
35 B. G. Johnson, P. M. W. Gill and J. A. Pople, *J. Chem. Phys.*, 1993, **98**, 5612.
36 C. W. Murray, G. J. Laming, N. C. Handy and R. D. Amos, *Chem. Phys. Lett.*, 1992, **199**, 551.
37 J. G. Rodriguez, F. H. Cano and S. Garcia-Blanco, *Cryst. Struct. Commun.*, 1979, **8**, 53.
38 G. J. Palenik and K. R. Dymock, *Acta Crystallogr.*, *Sect. B*, 1980, **36**, 2059.
39 J. G. Contreras, F. W. B. Einstein and D. G. Tuck, *Can. J. Chem.*, 1974, **52**, 3793.
40 R. L. Beddoes, D. R. Eardley, F. E. Mabbs, D. Moorcroft and M. A. Passand, *Acta Crystallogr.*, *Sect. C*, 1993, **49**, 1923.
41 H. Soling, *Acta Chem. Scand.*, *Ser. A*, 1976, **30**, 163.
42 N. W. Alcock, I. A. Degnan, S. M. Roe and M. G. H. Wallbridge, *J. Organomet. Chem.*, 1991, **414**, 285.
43 J. W. Akitt, in *Multinuclear NMR*, ed. J. Mason, Plenum Press, New York, 1987, p. 259.
44 A. Abragam, *The Principles of Nuclear Magnetism*, Oxford University Press, Oxford, 1961, p. 314.
45 M. Bühl, G. Hopp, W. v. Philipsborn, S. Beck, M.-H. Prosenc, U. Rief and H.-H. Brintzinger, *Organometallics.*, 1996, **15**, 778.
46 J. J. Dechter, U. Henriksson, J. Kowalewski and A.-C. Nilsson, *J. Magn. Reson.*, 1982, **48**, 503.
47 J. M. Aramini, D. D. McIntyre and H. J. Vogel, *J. Am. Chem. Soc.*, 1994, **116**, 11 506.
48 C. Cerny, J. Machacek, J. Fusek, O. Kriz, B. Casensky and D. G. Tuck, *J. Organomet. Chem.*, 1993, **456**, 250.

Received 6*th November* 1997; *Paper* 7/07986I